Clays Clay Miner., Vol. 71, No. 1:1–13, 2023
https://doi.org/10.1007/s42860-023-00229-5

ORIGINAL PAPER

Anomalous Viscosity, Aggregation, and Non-Ergodic Phase of Laponite® RD in a Water–Methanol Binary Solvent

Preeti Tiwari · Himadri B. Bohidar · Avik Das · Jitendra Bahadur · Najmul Arfin

Accepted: 6 April 2023 / Published online: 4 May 2023

Abstract Study of the behavior of landfill lining materials (clays) in organic solvents is important because, in waste management, lining prevents groundwater contamination by the adsorption of various pollutants such as chemicals and organic solvents. Although scaling behavior and the self-association property of clays in water-alcohol binary solvents have been studied by many researchers, the anomalous behavior of Laponite XLG in binary solvents requires investigation as suggested by previous studies. In the present study, Laponite® RD, which is structurally similar to Laponite XLG, was used to gain further insight into the reasons for the anomalous viscosity, aggregation, and non-ergodic behavior of clay in a water–methanol binary solvent. Dynamic light scattering (DLS) revealed the emergence of the non-ergodic phase of 3% w/v Laponite® RD in the water–methanol binary solvent, which increased in the presence of a large methanol content as well as with aging time in the binary solvent. Viscosity measurements further indicated that aggregation was responsible for the non-ergodic behavior, and small-angle X-ray scattering (SAXS) revealed that a large methanol content enhanced the aggregation. Moreover, SAXS data also revealed that the surface charge was responsible for anomalous viscosity fluctuations in the binary solvent due to interparticle repulsion within aggregates. Rheological studies showed that the large methanol content in the binary solvent led to frequency-independent behavior of the storage modulus of Laponite® RD.

Keywords Aggregation · Anomalous viscosity · Laponite · Non-ergodicity · Scattering

Associate Editor: Geoffrey Bowers.

P. Tiwari · N. Arfin (✉)
Soft Condensed Matter Laboratory, Centre for Interdisciplinary Research in Basic Sciences, Jamia Millia Islamia, New Delhi, India 110025
e-mail: narfin@jmi.ac.in

H. B. Bohidar
School of Physical Sciences, Jawaharlal Nehru University, New Delhi, India 110067

A. Das · J. Bahadur
Solid State Physics Division, Bhabha Atomic Research Centre, Trombay, Mumbai, India 400085

J. Bahadur
Homi Bhabha National Institute, Anushaktinagar, Mumbai, India 400094

Introduction

Clay minerals such as Laponite and montmorillonite (Mnt) have interesting phase states, e.g. glassy phase and gel phase, that occur as a function of clay concentration and aging time in a solution (Bonn et al., 1999; Jabbari-Farouji et al., 2008; Mourchid et al., 1998; Pujala et al., 2015; Ruzicka & Zaccarelli, 2011; Ruzicka et al., 2006). The various phase states, aging behavior, route of gelation, and gelation kinetics of clays have been reported extensively by many authors (Abou et al., 2001; Bandyopadhyay et al., 2004; Joshi et al., 2008; Knaebel et al., 2000; Kroon

et al., 1996; Mourchid & Levitz, 1998; Mourchid et al., 1995; Pujala et al., 2011b; Ranganathan & Bandyopadhyay, 2017; Ruzicka et al., 2004, 2010). Various techniques such as dynamic light scattering (DLS) (Arfin & Bohidar, 2014; Bellour et al., 2003; Kretzschmar et al., 1998; Nicolai & Cocard, 2000; Pujala & Bohidar, 2013), small angle X-ray scattering (SAXS) (Li et al., 2005; Mori et al., 2001; Morvan et al., 1994; Pignon et al., 1997a), small angle neutron scattering (SANS) (Avery & Ramsay, 1986; Pignon et al., 1998; Ramsay & Lindner, 1993), refractometry (Ravi Kumar et al., 2008), and rheology (Chang et al., 1993; Keren, 1989; Luckham & Rossi, 1999; Neaman & Singer, 2000; Pignon et al., 1997b; Ramsay, 1986; Rao, 2010; Teh et al., 2009) have been used to understand the behavior of clays in various solvents. Clays have been used for a wide range of biomedical applications such as bio-sensing (Mousty, 2010), bioimaging (Ding et al., 2016; Mornet et al., 2004), tissue engineering (Mihaila et al., 2014; Reffitt et al., 2003), delivery of regenerative microenvironments (Dawson et al., 2011), 3D cell printing for skeletal applications (Ahlfeld et al., 2017), drug delivery (Chen et al., 2015; Gonçalves et al., 2014; Wang et al., 2013; Wu et al., 2014; Zhuang et al., 2017), and many more (Chrzanowski et al., 2013; Kim et al., 2016; Rodrigues et al., 2013; Tomás et al., 2017).

Apart from biomedical applications, clays have been used in the paint industry (Seydibeyoglu et al., 2017), water purification (Annan et al., 2018; Brown et al., 2021), packaging coatings (Chandio et al., 2021), pollution remediation associated with gasoline (Sentenac et al., 2007), and waste management as clay liners (Alther, 1983, 1987; Anderson, 1982; Broderick & Daniel, 1990; Fernandez & Quigley, 1991). A clay-based liner system can minimize groundwater contamination by restricting pollutant migration. During the period of operation, the liner system may encounter various types of pollutants, chemicals, and organic solvents such as phenols, alcohols, etc. The exposure to organic solvents may affect the clay-based liner system and thus hamper its effectiveness and efficiency in ways that differ from estimates based on laboratory conditions. Researchers have thus tried to understand the effect of various organic solvents on clays. Sentenac et al. (2012) studied the effect of gasoline and diesel additives (ethanol and methyl-t-butyl ether) on kaolinite. A hybrid process of clay adsorption that removed soluble organics such as phenol and o-cresol from the water was studied by Lin et al. (2006). The macro and microstructure of Na-bentonite in the presence of methanol, acetone, acetic acid, and citric acid were studied by Goodarzi et al. (2016).

Although clays that are used as geosynthetic clay liners are almost exclusively natural clays with various chemical or physical modifications, the anomalous behavior of the synthetic clay, Laponite XLG, in a binary solvent and the unknown reason for some of the anomalous behavior were studied by Kimura and Haraguchi (2017). Researchers have tried to understand the effect of alcohol on clays; the literature on this topic is scarce, however, and among the few studies available, Permien and Lagaly (1994) discussed the formation of a band-type network in clay particles in a water-alcohol binary solvent. Those authors stated that band networks were shown to undergo contraction to form thicker particle aggregates at greater alcohol contents in water-alcohol binary mixtures. The scaling behavior of physical properties, i.e. zeta potential, hydrodynamic radius, viscosity, and surface tension of Laponite and montmorillonite in water-alcohol binary mixture was investigated by Pujala et al. (2011a). They noticed that the scaling behavior was independent of the aspect ratio of the different types of clays, though the scaling behavior was dependent on the solvent polarity. The self-association of clay minerals in water-alcohol binary mixtures was discussed by Pawar and Bohidar (2009) who revealed that the structure formation depends on the hydrophobicity of the solvent. The cluster formation phenomenon in Laponite which resulted from using oil instead of alcohol was explored by Garcia and Whitby (2012) who studied the breaking and recovery of the structure of the Laponite in an oil-in-water emulsion. An anomalous increase in the viscosity of Laponite XLG in water-alcohol binary solvents occurs when the alcohol used is ethanol, propanol, or butanol but does not occur with methanol (Kimura & Haraguchi, 2017). The phase diagram of Laponite in an alcohol-water binary mixture using real space imaging techniques and mechanical-strength techniques was investigated by Pujala and Bohidar (2019).

The objective of the present study was to investigate further the viscosity behavior of Laponite® RD in a water–methanol binary solvent, using small-angle X-ray scattering, and compare the results with

https://doi.org/10.1007/s42860-023-00229-5 Published online by Cambridge University Press

those observed by Kimura and Haraguchi (2017) for Laponite® XLG. It was assumed that both Laponite® RD and Laponite® XLG will behave similarly because of their structural similarities and gel-forming capacity, irrespective of the few dissimilarities between them. Laponite® XLG is a high-purity form of Laponite® RD and is commonly employed in biomedical applications as it has small heavy metal content and shows very little toxicity (Cummins, 2007; Tomás et al., 2017). The hypothesis was that the viscous behavior of Laponite® RD would be in accord with Laponite® XLG and that the viscosity fluctuations are due to interparticle repulsion between charged Laponite surfaces within the aggregates.

Materials and Methods

Laponite® RD (BYK-Additives Ltd., UK) was received as a gift from Aroma Chemical Agencies (India) Pvt. Ltd, New Delhi, India. Methanol with a purity of 99.7% was purchased from Merck (Darmstadt, Germany).

Laponite is a hygroscopic material that can absorb moisture from the environment which adds to its weight and leads to inconsistency during sample preparation. Therefore, to remove excess moisture and obtain uniform dispersions in aqueous solutions, Laponite® RD powder was dried in an oven at 50°C for 8–10 h. Dried Laponite® RD (0.45 g) was then stirred and dissolved in 5 mL, 12.5 mL, 10 mL, and 7.5 mL of deionized water, using a magnetic stirrer, until the suspension was clear. Different volumes of methanol were added and stirred immediately to the above aqueous Laponite® RD suspensions, to make up the final volume of the solution to 15 mL until a 3% w/v Laponite® RD in water–methanol binary solvent was obtained with various water:methanol (W:M) ratios, i.e. 1:0, 5:1, 2:1, and 1:1 (v/v). The samples were prepared at room temperature, nominally 25°C.

Dynamic light scattering, SAXS, and viscosity measurements were carried out to study the time-dependent behavior of samples. The storage and loss modulus of the samples were studied using a rheometer.

The DLS study was performed using a Zetasizer Nano ZS (Malvern Panalytical, Worcestershire, UK). The light scattering technique is often used to study ergodic and non-ergodic systems. Ergodic systems are those where the time average description is similar to its ensemble average property. However, in the arrested phase (a phase in which the particles do not execute Brownian motion due to restrictions in movements caused by jamming and/or crowding), the ergodicity condition may fail, resulting in a non-ergodic system. The scattering centers in non-ergodic systems are localized near fixed mean positions and execute restricted Brownian motion. The condition of non-ergodicity results in the failure of the Siegert relation given by Eq. 1.

$$g_2(\tau) = 1 + \beta(|g_1(\tau)|^2) \quad (1)$$

where, $g_2(\tau)$ is the intensity correlation function, β is the coherence factor, and $g_1(\tau)$ is the field correlation function.

The issue of non-ergodicity was thus resolved using Eq. 2 as mentioned by Coviello et al. (1997):

$$g_2(\tau) = 1 + \beta'[2X(1-X)g_1(\tau) + X^2\left(|g_1(\tau)|^2\right)] \quad (2)$$

where β' is the coherence factor and has a maximum value of 1 and X is the ergodic parameter.

The SAXS experiments were carried out at the SWAXS beamline (BL-18) of the Indus-2 synchrotron at Raja Ramanna Centre for Advanced Technology (RRCAT), Indore, India. BL-18 is a bending magnet (1.5 T)-based synchrotron beam line facility which is equipped with a double-crystal monochromator (pair of flat Si [111] crystals) to tune the monochromatic X-ray energy in the range of 5–20 keV with a resolution of ~10^{-3} keV. A 1.5 m long toroidal X-ray mirror (60 nm Pt and 5 nm Rh coating on a silicon substrate) was used to focus the monochromatic X-ray beam onto the detector plane. The SAXS data, using monochromatic X-rays of 16 keV (wavelength ~ 0.77 Å) were collected on a 2D online image plate (mar 345) detector keeping the sample-to-detector distance at ~3.2 m. The background noise and the empty cell scattering signal with an estimated transmission factor were subtracted from the raw SAXS data before further processing. The viscosity of samples was measured by a sine wave vibro-viscometer (SV: 10–100, A&D Co. Ltd., Tokyo, Japan). All the viscosity readings were recorded at the interval of 5 s. The rheology experiment was carried out using

https://doi.org/10.1007/s42860-023-00229-5 Published online by Cambridge University Press

an AR-500 model stress controller rheometer (T.A. Instruments, Cheshire, UK). The elastic modulus of samples was measured by cone-plate geometry (2 cm diameter, 2° cone angle) with the oscillation stress value set at 0.1 Pa. The study was used to determine the frequency-dependent storage modulus in the frequency range 0.1–100 rad/s.

Results and Discussion

Dynamic Light Scattering (DLS)

The aging behavior in soft matter systems is usually probed by scattering experiments through dynamic-structure factor and correlation-curve analysis. The correlation function (Fig. 1) showed the emergence of non-ergodic behavior of Laponite® RD (3% w/v) in a water–methanol binary solvent as a function of methanol content and aging time.

The issue of non-ergodicity in DLS experiments is understood by scanning the entire phase space of the sample cell via rotation (Coviello et al., 1997). Nevertheless, the heterodyne approach (Coviello et al., 1997) can also be implemented to understand the non-ergodic system using Eq. 2. The value of $X=1$ in Eq. 2 transforms it into Eq. 1 where the Siegert relation holds; whereas, for the non-ergodic phase, the value of $X<1$ and the term $2X(1-X)$ makes a finite contribution to $g_2(\tau)$. The pre-factor of the linear term for $g_1(\tau)$ in Eq. 2 was observed to be much larger than the quadratic second term in most of the cases and thus $g_1(\tau)$ can be written as Eq. 3:

$$g_1(\tau) \approx [g_2(\tau) - 1]/[2\beta'(X(1-X))] \quad (3)$$

The intercept of the plot of $[g_2(\tau) - 1]$ *vs.* delay time, τ, at $\tau \to 0$ gives $\beta'[2X - X^2]$ from which the value of X was calculated.

The calculated value of the ergodic parameter, X, was plotted (Fig. 2) and the value of X for Laponite® RD in the binary solvent decreased with aging as well as with the increase in methanol content. The plot of

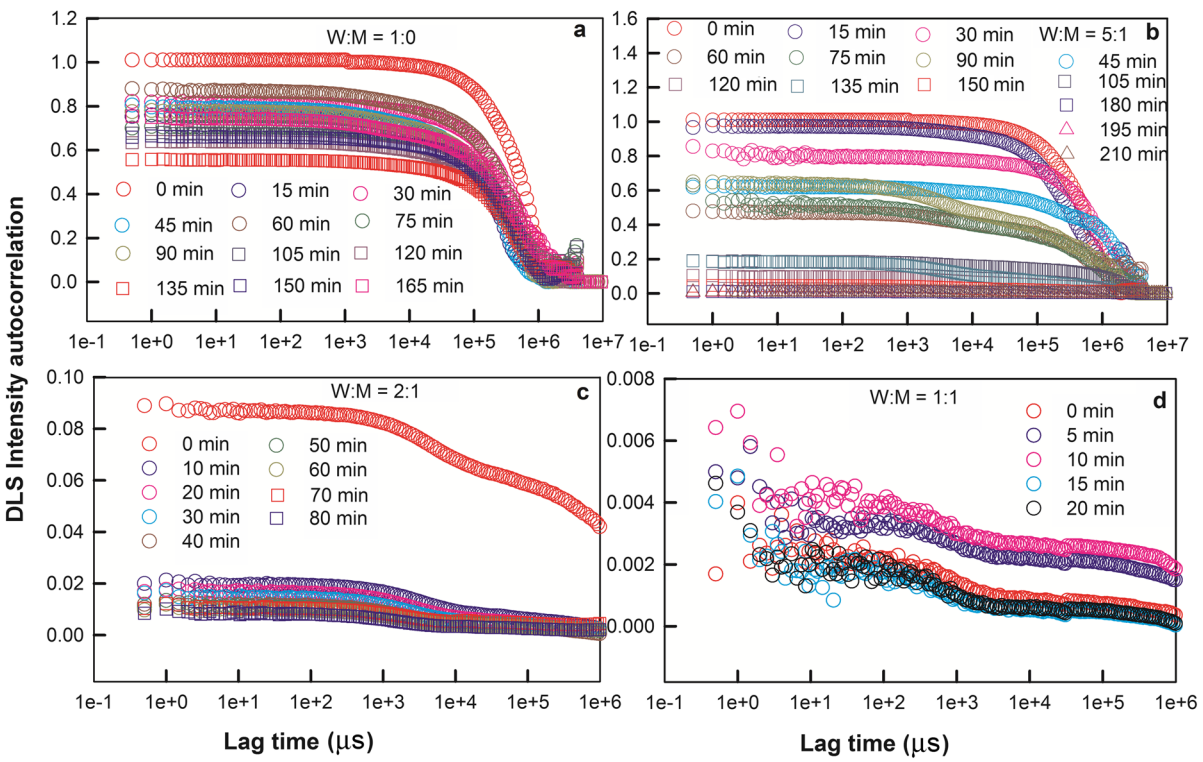

Fig. 1 Intensity autocorrelation curve of 3% w/v Laponite® RD in a water–methanol binary solvent for various W:M ratios: **a** 1:0, **b** 5:1, **c** 2:1, and **d** 1:1

https://doi.org/10.1007/s42860-023-00229-5 Published online by Cambridge University Press

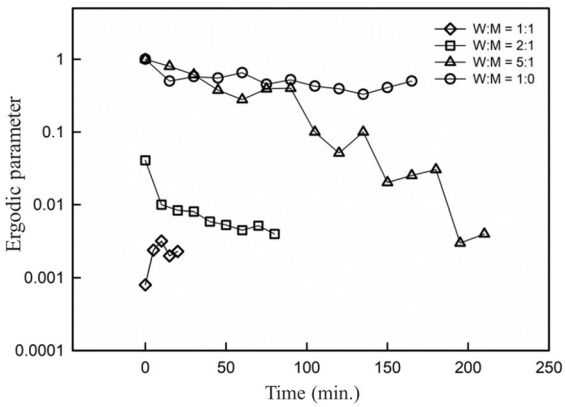

Fig. 2 Variation of the ergodic parameter (X) as a function of time for 3% w/v Laponite® RD in various W:M ratios: **a** 1:0, **b** 5:1, **c** 2:1, and **d** 1:1

X (Fig. 2) suggested that the sample with a W:M = 1:0 ratio remained ergodic until 165 min whereas samples with a larger methanol content became non-ergodic at a much earlier time.

Viscosity Measurement

Viscosity studies were used to determine the evolution of the non-ergodic behavior of Laponite® RD in the binary solvent. The viscosity data (Fig. 3a) showed that initially ($t \approx 0$ min) the relative viscosity was very small for Laponite® RD in W:M = 1:0; with aging, however, the viscosity increased. The increase in viscosity led to the formation of a gel with a house-of-cards arrangement. As discussed in various previous studies (Cummins, 2007; Martin et al., 2002; Mongondry et al., 2005; Ruzicka et al., 2004; Shahin & Joshi, 2010), the house-of-cards arrangement was formed due to the interaction between the negatively charged surfaces and positively charged edges of Laponite® RD in a high ionic-strength solution. The assertion of the house-of-cards arrangement, however, was derived from the work of Shahin and Joshi (2010) who suggested that the aging that occurs over a long period of time in a low salt-concentration system is qualitatively

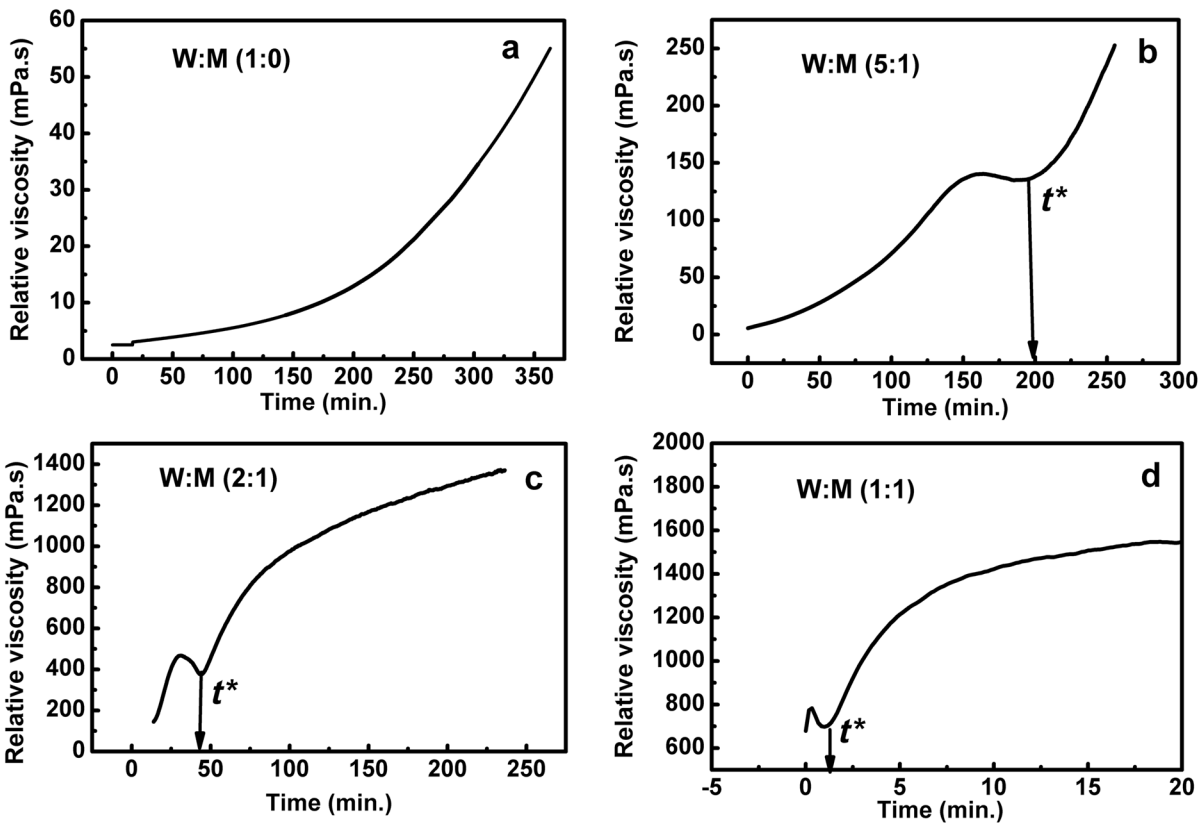

Fig. 3 Time-dependent viscosity of 3% w/v Laponite® RD in a water–methanol binary solvent for various W:M ratios: **a** 1:0, **b** 5:1, **c** 2:1, and **d** 1:1. The arrow indicates the time, t^*, where viscosity fluctuation was observed

https://doi.org/10.1007/s42860-023-00229-5 Published online by Cambridge University Press

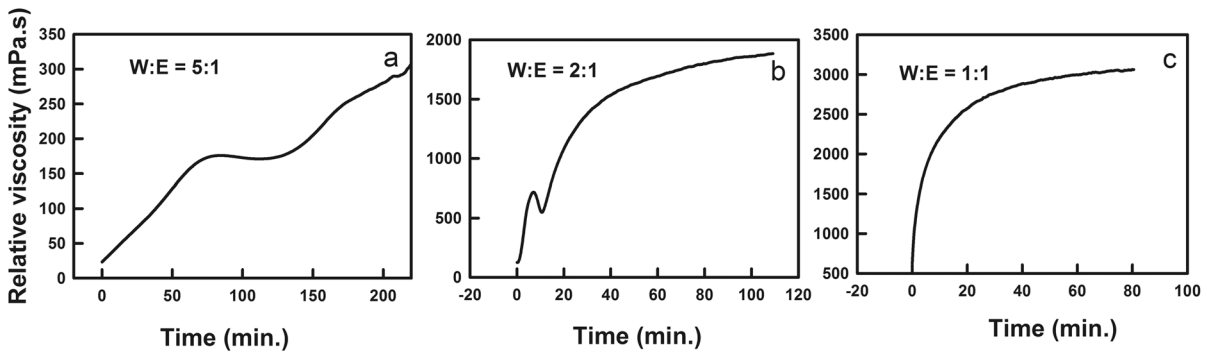

Fig. 4 Time-dependent viscosity of 3% w/v Laponite® RD in a water–ethanol binary solvent with various water:ethanol ratios: **a** 5:1, **b** 2:1, and **c** 1:1

similar to that occurring in high salt-concentration systems over a short period of time.

The plot of viscosity vs time (Fig. 3) suggested that the relative viscosity (at $t \approx 0$ min) for 3% w/v Laponite® RD in the binary solvent increased with the increase in methanol content. This increase was attributed to the aggregation of Laponite® RD particles owing to the limited availability of water for hydration. Note that the viscosity trend of Laponite® RD for W:M ratios of 1:0 and 5:1 (Fig. 3a,b) was evolving whereas the saturated viscosity profile was observed for W:M ratios of 2:1 and 1:1 (Fig. 3c,d). The data indicated that the large viscosity value and the plateau region may have evolved due to the aggregation of particles because of jamming and limited access to water for hydration.

Nevertheless, in the viscosity profile (Fig. 3b, c, d), an anomaly was noted at time t^* at which a reduction in viscosity was observed. The anomalous fluctuation in viscosity at t^* and a plateau region for large alcohol contents in binary solvents was not an artefact; in fact, the anomalous fluctuation and plateau region could invariably be seen in binary mixtures when ethanol was used instead of methanol (Fig. 4). An anomalous viscosity fluctuation by Laponite XLG in a water-alcohol binary mixture was also observed by Kimura and Haraguchi (2017).

Small-angle X-ray Scattering (SAXS)

Viscosity measurements revealed the occurrence of aggregation in Laponite® RD particles with the passage of time and increasing methanol concentration in the binary solvent. Nothing definitive could be stated about the viscosity fluctuations, i.e. the reduction in the viscosity measurements. This suggests that the reduction was due to repulsion between negatively charged Laponite® RD surfaces within the aggregates. This hypothesis of aggregation and repulsion behavior within aggregates was supported by results from the SAXS study. The plot (Fig. 5) depicted the scattering intensity (I) profile of Laponite® RD in a water–methanol binary solvent as a function of scattering vector (q) for various W:M ratios immediately after sample preparation, i.e. $t=0$. The SAXS data (Fig. 5) revealed that the scattering profile could be split into two regions, referred to here as I and II. The data points in region II for all

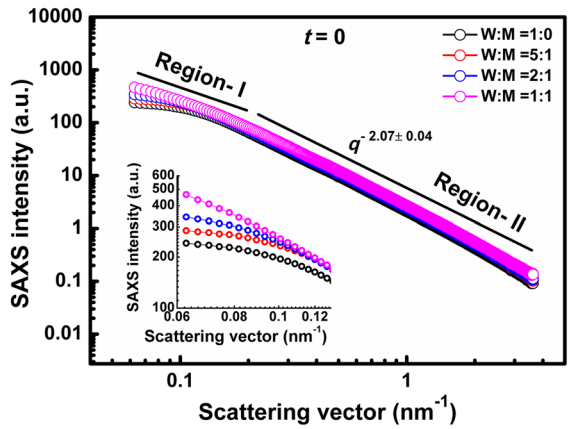

Fig. 5 SAXS scattering intensity (I) profile of 3% w/v Laponite® RD in a water–methanol binary solvent as a function of scattering vector (q) for various W:M ratios at the initial time ($t=0$). Inset is a close-up image of region I

https://doi.org/10.1007/s42860-023-00229-5 Published online by Cambridge University Press

samples could be fitted with the power law $I \approx q^{-\alpha}$ where the value of $\alpha = 2.07 \pm 0.04$. The value of 2 for α in the high-q region (region II) suggested that the Laponite® RD particle is disc-shaped (Cui et al., 2013). Data from the low-q region (region I) revealed that scattering intensity from Laponite® RD increased with the increase in methanol concentration in the binary solvent (see inset in Fig. 5). The increase in scattering intensity suggested enhanced aggregation of Laponite® RD in samples with increasing methanol content (Chatani et al., 2015; Kikhney & Svergun, 2015; Lecomte et al., 2000; Londoño et al., 2018).

The data (Fig. 5) showed a variation (immediately after sample preparation, i.e. $t = 0$) of scattering intensity as a function of the scattering vector; the data, however, revealed nothing about the anomalous fluctuation that occurred with the passage of time. The aging behavior was observed from the time-dependent scattering intensity of the SAXS profile of each individual sample (Fig. 6); apparently the scattering profile was the same with aging for larger q values; at smaller q values, however, some variations were noticed.

The explicit variation of the scattering profile with aging time at low q (0.0627 nm^{-1}) revealed the interactions between Laponite® RD particles in the water–methanol binary solvents. The variation of scattering intensity for each sample at $q = 0.0627$ nm^{-1} as a function of time (Fig. 7b, c, d) revealed that the

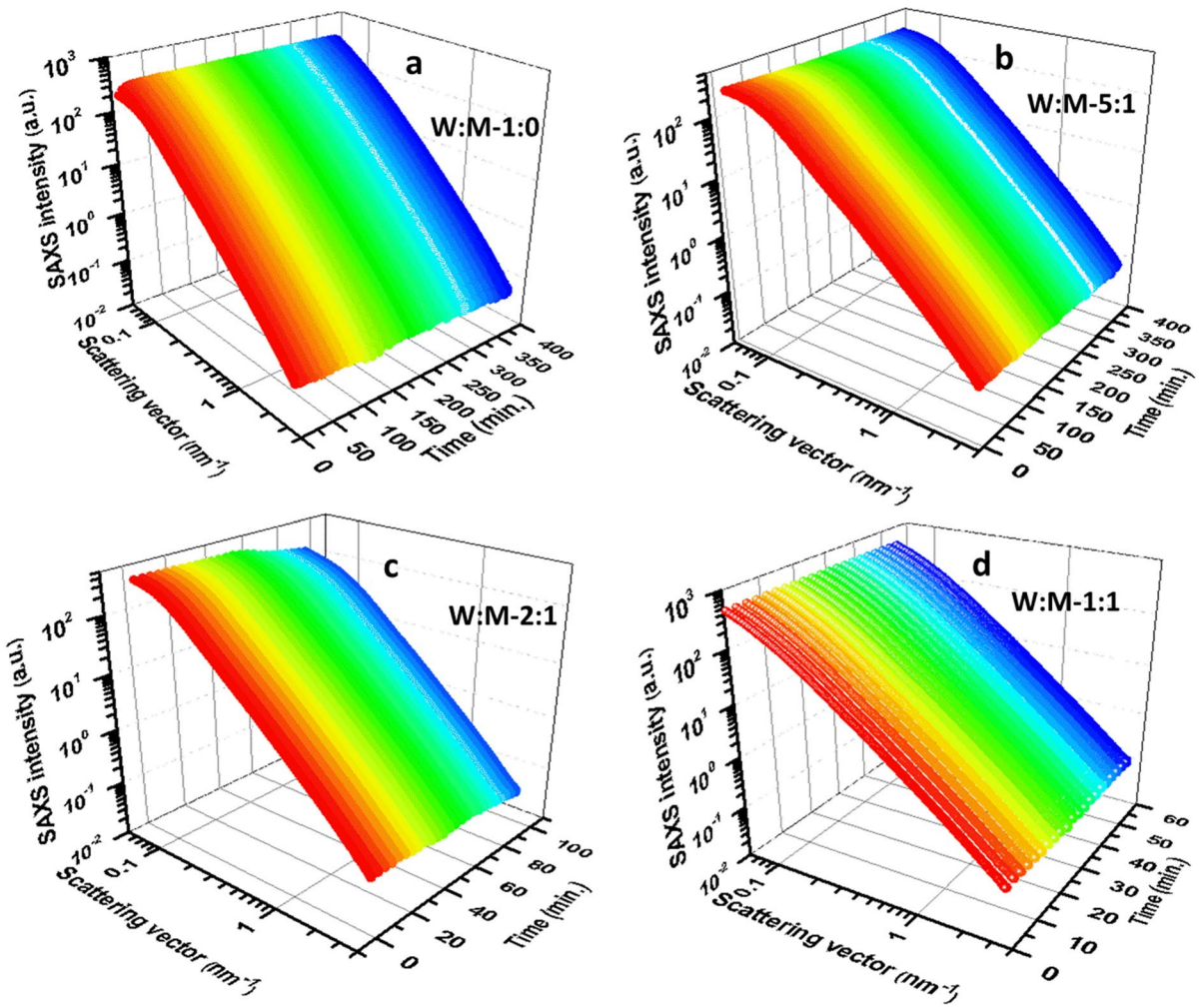

Fig. 6 SAXS intensity (I) profile as a function of the scattering vector (q) and aging time for 3% w/v Laponite® RD in a water–methanol binary mixture at various W:M ratios

https://doi.org/10.1007/s42860-023-00229-5 Published online by Cambridge University Press

scattering intensity decreased with aging in all the samples with methanol, which suggests a repulsive interaction (Franke et al., 2012; Kikhney & Svergun, 2015) between Laponite® RD particles. The repulsive force within aggregates might be the reason for the observed anomalous fluctuation (reduction in viscosity) as mentioned in the viscosity section (Fig. 3).

The sample without methanol (W:M = 1:0) showed an increase in scattering intensity with time (Fig. 7a), which suggested an attractive interaction (Franke et al., 2012; Kikhney & Svergun, 2015) between the negatively charged basal surface and the positively charged edge of the Laponite® RD, thus forming the house-of-cards arrangement discussed above.

Note that the rise in viscosity of Laponite® RD in water–methanol binary solvent as observed in this work was not in accord with the results obtained by Kimura and Haraguchi (2017); those authors did not note an anomalous increase in the viscosity of Laponite XLG in water–methanol binary solvents. Although both Laponite® RD and Laponite XLG are structurally similar and have gel-forming properties, the difference in the results may be attributed to the sample preparation. Kimura and Haraguchi (2017) prepared samples by adding alcohol in a dropwise manner whereas in the current study methanol was added immediately during the preparation of samples. The sudden and immediate addition of methanol may have contributed to the sudden flocculation and aggregation of Laponite® RD, which was responsible for the anomalous increase in the viscosity. The occurrence of dissimilar anomalous behavior among different grades of Laponite in water-alcohol binary solvents needs meticulous investigation, considering various parameters, such as purity, heavy-metal content, extent of exfoliation, and hydration behavior, as mentioned by Kimura and Haraguchi (2017).

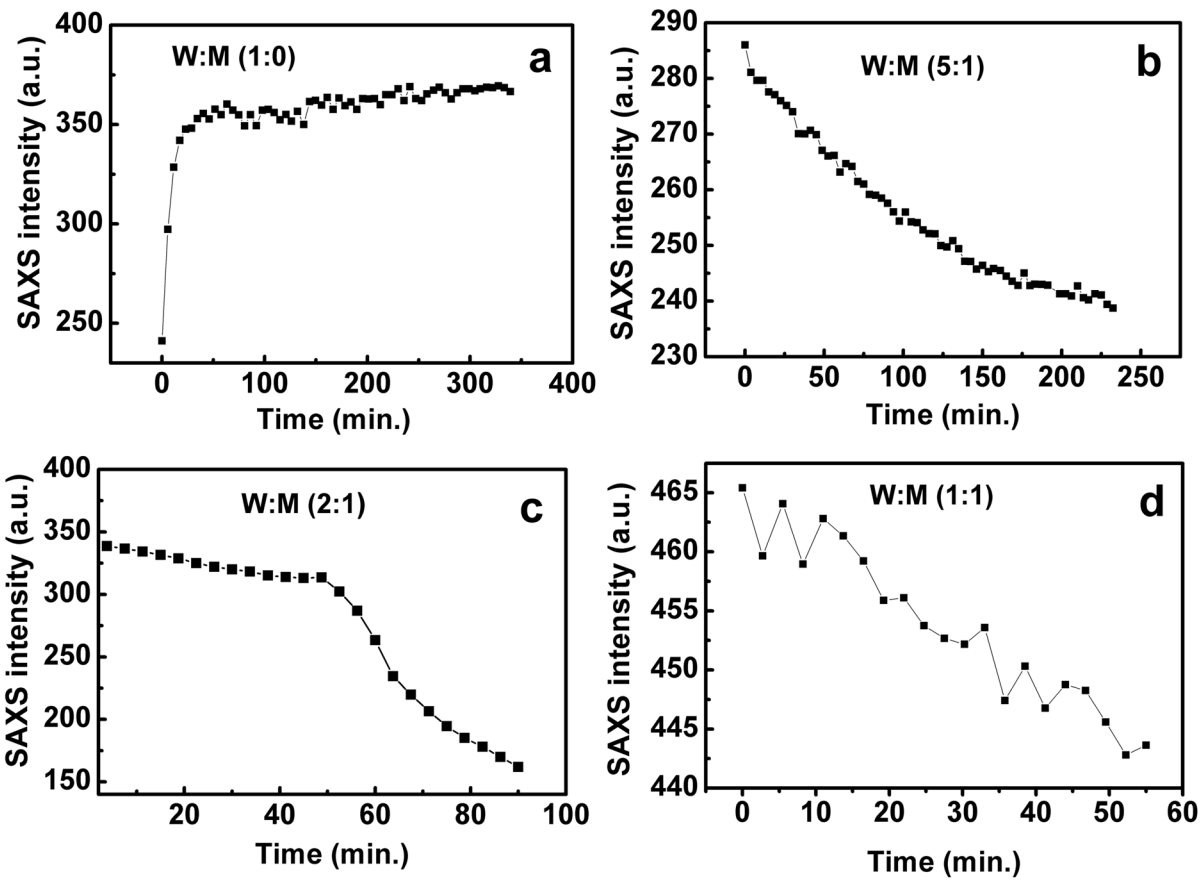

Fig. 7 SAXS intensity (I) profile of Laponite® RD as a function of time at the lowest scattering vector ($q = 0.0627$ nm^{-1}) for various W:M ratios

https://doi.org/10.1007/s42860-023-00229-5 Published online by Cambridge University Press

The observed time-dependent fluctuation in the viscosity of Laponite® RD in a water-alcohol binary solvent was, however, in accord with the results obtained by Kimura and Haraguchi (2017). The SAXS data revealed that the repulsive forces due to negatively charged Laponite® RD platelets within aggregates were the reason for such anomalous viscosity fluctuations.

Rheology

The viscoelastic properties of the samples were characterized using rheology. The samples were allowed to mature for 30 h before performing the rheological experiments. The storage modulus ($G'(\omega)$) and loss modulus ($G''(\omega)$) of the samples were plotted (Fig. 8) to characterize the viscoelastic properties. The explicit frequency dependence of the storage modulus was determined by fitting $G'(\omega)$ to the power-law function given by Eq. 4 (Barnes, 2000).

$$G'(\omega) \sim \omega^{n} \tag{4}$$

where ω is the angular frequency.

The data (Fig. 8) showed the frequency-dependent storage and loss modulus of 3% w/v Laponite® RD in a binary solvent with W:M ratios of 1:0, 5:1, 2:1, and 1:1. The data (Fig. 8) revealed that the interaction between Laponite® RD particles increased with high methanol concentrations, which gave rise to a

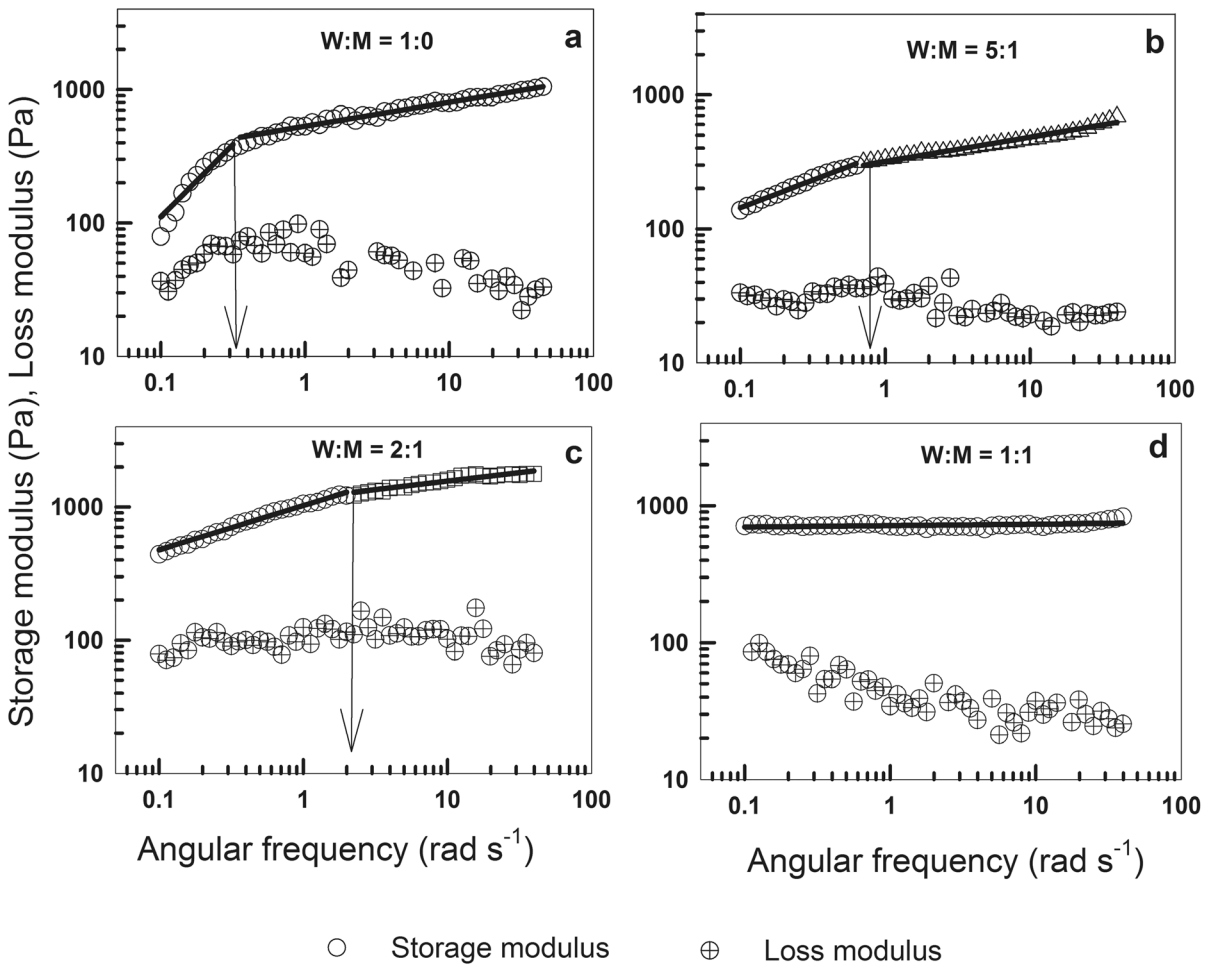

Fig. 8 Variation of storage modulus ($G'(\omega)$) and loss modulus ($G''(\omega)$) as a function of frequency for 3% w/v Laponite® RD in a water–methanol binary solvent with various W:M ratios: **a** 1:0, **b** 5:1, **c** 2:1, and **d** 1:1. The arrow indicates the frequency at which the slope of the storage modulus changed

https://doi.org/10.1007/s42860-023-00229-5 Published online by Cambridge University Press

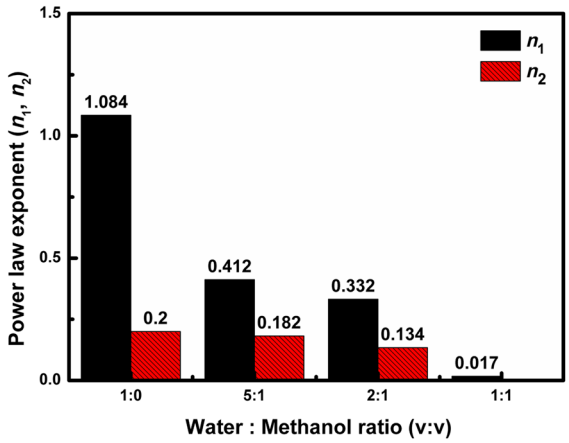

Fig. 9 Variation in the power law exponents (n_1 and n_2) for 3% w/v Laponite® RD in a water–methanol binary solvent with various W:M ratios: **a** 1:0, **b** 5:1, **c** 2:1, and **d** 1:1

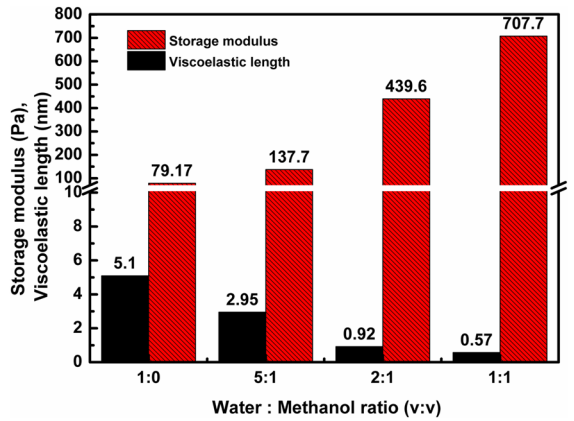

Fig. 11 Variation of the storage modulus (G_0 (ω)) at 0.1 rad/s and viscoelastic length (ζ) for 3% w/v Laponite® RD in a water–methanol binary solvent with various W:M ratios: **a** 1:0, **b** 5:1, **c** 2:1, and **d** 1:1

large storage modulus. Furthermore, the storage modulus exhibited two regions (indicated by the arrow) based on the slope of the graph except for the case when W:M = 1:1. The two regions were fitted to Eq. 4 which gave two power law exponents n_1 and n_2.

The linear viscoelastic model (Barnes, 2000) predicts that the power-law frequency dependence behavior given by Eq. 4 with $0 < n < 1$ will be followed. The number of crosslinks (excess crosslinks, $n < 1/2$ and lack of crosslinks, $n > 1/2$) defines stoichiometric balanced and unbalanced networks strictly for chemically crosslinked gels. The data (Fig. 8) were, however, fitted to Eq. 4 and the value of n was determined in order to understand the strength of the samples.

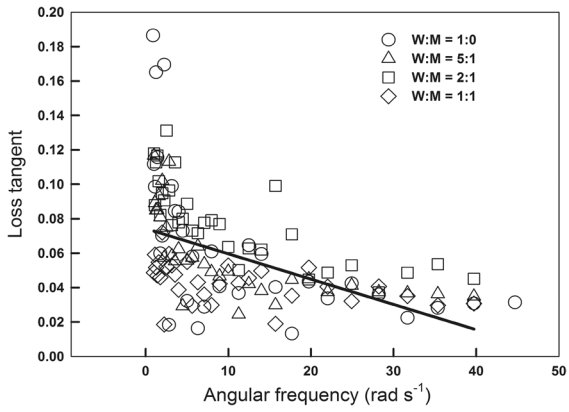

Fig. 10 Variation of the loss tangent (tan δ) as a function of frequency for Laponite® RD in a water–methanol binary solvent with W:M ratios of 1:0, 5:1, 2:1, and 1:1. The straight line in the graph shows a single fitting to all the data points

The power law exponents (n_1 and n_2) were obtained and plotted (Fig. 9) by fitting the storage modulus data (Fig. 8) using Eq. 4. From the large storage modulus (Fig. 8) and almost zero frequency dependence (Fig. 9) for W:M = 1:1, the present authors concluded that a high concentration of methanol provided greater physical interaction between Laponite® RD particles.

Furthermore, understanding whether Laponite® RD in the binary solvent has gel or melt-like behavior is important. In order to understand the arrested phase, a plot of the loss tangent ($\tan\delta = G''(\omega)/G'(\omega)$) as a function of frequency (Fig. 10) for various W:M ratios yielded a straight-line equation ($\tan\delta = 0.07 - 0.001\ \omega$) of almost zero slope, indicating that Laponite® RD aggregates in binary solvent behaved almost like a gel in all the samples.

The low-frequency storage modulus, G_0, defined as $G_0 = \lim_{\omega \to 0} G'(\omega)$ was determined explicitly using Eq. 5 (Arfin et al., 2014; Barnes, 2000). The equation gave the measure of elastic free energy stored per unit volume of a characteristic viscoelastic network of size ζ (Barnes, 2000).

$$\zeta^3 \approx k_B T / G_0 \tag{5}$$

The value of G_0 for each sample in this work was determined at 0.1 rad/s. The values for G_0 and viscoelastic length (ζ) obtained from Eq. 5 were

https://doi.org/10.1007/s42860-023-00229-5 Published online by Cambridge University Press

plotted (Fig. 11) and indicated that the rigidity of the Laponite® RD network increased with the increase in methanol concentration in the binary solvent.

Conclusions

The non-ergodic behavior and viscosity of Laponite® RD in a water–methanol binary solvent increased strongly with aging time and methanol content. The increase in viscosity was attributed to the aggregation of Laponite® RD particles as revealed through the SAXS experiment. The hypothesis that the fluctuation in the viscosity behavior occurred due to the repulsion between negatively charged Laponite® RD surfaces within the aggregates is consistent with the analysis of the SAXS. Nevertheless, the results obtained are at variance with the results obtained for Laponite XLG (Kimura & Haraguchi, 2017) which showed no significant increase in viscosity in the water–methanol binary solvent.

Acknowledgements Ms Preeti Tiwari is grateful to the Council of Scientific and Industrial Research (CSIR) for the CSIR-SRF fellowship (09/466(0222))/2019-EMR-I. The authors are also grateful to the UGC start-up grant (F.30-359/2017(BSR)) for funding. Avik Das and Jitendra Bahadur acknowledge Dr S. M. Yusuf, Director of Physics Group, Bhabha Atomic Research Centre, for his support and encouragement for the SAXS beamline (BL-18) activity. The authors also acknowledge Aroma Chemical Agencies (India) Pvt. Ltd. for the supply of Laponite® RD (BYK-Additives and Instruments, UK) and the Central Instrumentation Facility, Centre for Interdisciplinary Research in Basic Sciences, Jamia Millia Islamia, for the instrumentation facility.

Data Availability Not Applicable.

Code Availability Not Applicable.

Declarations

Conflicts of Interest There are no conflicts to declare.

References

Abou, B., Bonn, D., & Meunier, J. (2001). Aging dynamics in a colloidal glass. *Physical Review E, 64*, 021510.

Ahlfeld, T., Cidonio, G., Kilian, D., Duin, S., Akkineni, A. R., Dawson, J. I., Yang, S., Lode, A., Oreffo, R. O. C., & Gelinsky, M. (2017). Development of a clay based bioink for 3D cell printing for skeletal application. *Biofabrication, 9*, 034103.

Alther, G. R. (1983). The methylene blue test for bentonite liner quality control. *Geotechnical Testing Journal, 6*(3), 128–132.

Alther, G. R. (1987). The qualifications of bentonite as a soil sealant. *Engineering Geology, 23*, 177–191.

Anderson, D. C. (1982). Does landfill leachate make clay liners more permeable? *Civil Engineering, 52*(9), 66–69.

Annan, E., Agyei-Tuffour, B., Bensah, Y. D., Konadu, D. S., Yaya, A., Onwona-Agyeman, B., & Nyankson, E. (2018). Application of clay ceramics and nanotechnology in water treatment: A review. *Cogent Engineering, 5*(1), 1476017.

Arfin, N., & Bohidar, H. B. (2014). Ergodic-to-nonergodic phase inversion and reentrant ergodicity transition in DNA–nanoclay dispersions. *Soft Matter, 10*(1), 149–156.

Arfin, N., Aswal, V. K., & Bohidar, H. B. (2014). Overcharging, thermal, viscoelastic and hydration properties of DNA–gelatin complex coacervates: Pharmaceutical and food industries. *RSC Advances, 4*(23), 11705–11713.

Avery, R. G., & Ramsay, J. D. F. (1986). Colloidal properties of synthetic hectorite clay dispersions: II. Light and small angle neutron scattering. *Journal of Colloid and Interface Science, 109*(2), 448–454.

Bandyopadhyay, R., Liang, D., Yardimci, H., Sessoms, D. A., Borthwick, M. A., Mochrie, S. G. J., Harden, J. L., & Leheny, R. L. (2004). Evolution of particle-scale dynamics in an aging clay suspension. *Physical Review Letters, 93*(22), 228302.

Barnes, H. A. (2000). *A Handbook of Elementary Rheology*. University of Wales.

Bellour, M., Knaebel, A., Harden, J. L., Lequeux, F., & Munch, J. P. (2003). Aging processes and scale dependence in soft glassy colloidal suspensions. *Physical Review E, 67*, 031405.

Bonn, D., Kellay, H., Tanaka, H., Wegdam, G., & Meunier, J. (1999). Laponite: What is the difference between a gel and a glass? *Langmuir, 15*(22), 7534–7536.

Broderick, G. P., & Daniel, D. E. (1990). Stabilizing compacted clay against chemical attack. *Journal of Geotechnical Engineering, 116*(10), 1549–1567.

Brown, K., Mendoza, M., Tinsley, T., Bee-DiGregorio, M. Y., Bible, M., Brooks, J. L., Colorado, M., Esenther, J., Farag, A., Gill, R., Kalivas, E. N., Lara, R., Lutz, A., Nazaire, J., Mazo, A. R., Rodriguez, R. S., Schwabacher, J. C., Zestos, A. G., Hartings, M. R., & Fox, D. M. (2021). Polyvinyl alcohol-montmorillonite composites for water purification: Analysis of clay mineral cation exchange and composite particle synthesis. *Polyhedron, 205*, 115297.

Chandio, A. D., Channa, I. A., Rizwan, M., Akram, S., Javed, M. S., Siyal, S. H., Saleem, M., Makhdoom, M. A., Ashfaq, T., Khan, S., Hussain, S., Albaqami, M. D., & Alotabi, R. G. (2021). Polyvinyl alcohol and nano-clay based solution processed packaging coatings. *Coatings, 11*(8), 942.

Chang, S. H., Ryan, M. E., & Gupta, R. K. (1993). The effect of pH, ionic strength, and temperature on the rheology and stability of aqueous clay suspensions. *Rheologica Acta, 32*, 263–269.

Chatani, E., Inoue, R., Imamura, H., Sugiyama, M., Kato, M., Yamamoto, M., Nishida, K., & Kanaya, T. (2015). Early aggregation preceding the nucleation of insulin amyloid fibrils as monitored by small angle X-ray scattering. *Scientific Reports, 5*, 15485.

Chen, G., Li, D., Li, J., Cao, X., Wang, J., Shi, X., & Guo, R. (2015). Targeted doxorubicin delivery to hepatocarcinoma cells by lactobionic acid-modified laponite nanodisks. *New Journal of Chemistry, 39*, 2847–2855.

Chrzanowski, W., Kim, S. Y., & Neel, E. A. A. (2013). Biomedical applications of clay. *Australian Journal of Chemistry, 66*(11), 1315–1322.

Coviello, T., Burchard, W., Geissler, E., & Maier, D. (1997). Static and dynamic light scattering by a thermoreversible gel from *Rhizobium leguminosarum* 8002 Exopolysaccharide. *Macromolecules, 30*(7), 2008–2015.

Cui, Y., Pizzey, C. L., & van Duijneveldt, J. S. (2013). Modifying the structure and flow behavior of aqueous montmorillonite suspensions with surfactant. *Philosophical Transactions of the Royal Society A: Mathematical, Physical and Engineering Sciences, 371*(1988), 20120262.

Cummins, H. Z. (2007). Liquid, glass, gel: The phases of colloidal laponite. *Journal of Non-Crystalline Solids, 353*(41–43), 3891–3905.

Dawson, J. I., Kanczler, J. M., Yang, X. B., Attard, G. S., & Oreffo, R. O. C. (2011). Clay gels for the delivery of regenerative microenvironments. *Advanced Materials, 23*(29), 3304–3308.

Ding, L., Hu, Y., Luo, Y., Zhu, J., Wu, Y., Yu, Z., Cao, X., Peng, C., Shi, X., & Guo, R. (2016). Laponite® stabilized iron oxide nanoparticles for *in vivo* MR imaging of tumors. *Biomaterials Science, 4*(3), 474–482.

Fernandez, F., & Quigley, R. M. (1991). Controlling the destructive effect of clay-organic liquid interactions by application of effective stress. *Canadian Geotechnical Journal, 28*(3), 388–398.

Franke, D., Kikhney, A. G., & Svergun, D. I. (2012). Automated acquisition and analysis of small angle X-ray scattering data. *Nuclear Instruments and Methods in Physics Research A, 689*, 52–59.

Garcia, P. C., & Whitby, C. P. (2012). Laponite stabilised oil-in-water emulsions: Viscoelasticity and thixotropy. *Soft Matter, 8*(5), 1609–1615.

Gonçalves, M., Figueira, P., Maciel, D., Rodrigues, J., Qu, X., Liu, C., Tomás, H., & Li, Y. (2014). pH-sensitive Laponite®/doxorubicin/alginate nanohybrids with improved anticancer efficacy. *Acta Biomaterialia, 10*(1), 300–307.

Goodarzi, A. R., Fateh, S. N., & Shekary, H. (2016). Impact of organic pollutants on the macro and microstructure responses of Na-bentonite. *Applied Clay Science, 121–122*, 17–28.

Jabbari-Farouji, S., Tanaka, H., Wegdam, G. H., & Bonn, D. (2008). Multiple nonergodic disordered states in Laponite suspensions: A phase diagram. *Physical Review E, 78*(6), 061405.

Joshi, Y. M., Reddy, G. R. K., Kulkarni, A. L., Kumar, N., & Chhabra, R. P. (2008). Rheological behavior of aqueous suspensions of laponite: New insights into the ageing phenomena. *Proceedings of the Royal Society a: Mathematical, Physical and Engineering Sciences, 464*(2090), 469–489.

Keren, R. (1989). Effect of clay charge density and adsorbed ions on the rheology of montmorillonite suspension. *Soil Science Society of America Journal, 53*(1), 25–29.

Kikhney, A. G., & Svergun, D. I. (2015). A practical guide to small angle X-ray scattering (SAXS) of flexible and intrinsically disordered proteins. *FEBS Letters, 589*(19 Pt A), 2570–2577.

Kim, M. H., Choi, G., Elzatahry, A., Vinu, A., Choy, Y. B., & Choy, J. H. (2016). Review of clay-drug hybrid materials for biomedical applications: Administration routes. *Clays and Clay Minerals, 64*(2), 115–130.

Kimura, Y., & Haraguchi, K. (2017). Clay–alcohol–water dispersions: Anomalous viscosity changes due to network formation of clay nanosheets induced by alcohol clustering. *Langmuir, 33*(19), 4758–4768.

Knaebel, A., Bellour, M., Munch, J. P., Viasnoff, V., Lequeux, F., & Harden, J. L. (2000). Aging behavior of laponite clay particle suspensions. *Europhysics Letters, 52*(1), 73–79.

Kretzschmar, R., Holthoff, H., & Sticher, H. (1998). Influence of pH and Humic Acid on Coagulation Kinetics of Kaolinite: A Dynamic Light Scattering Study. *Journal of Colloid and Interface Science, 202*(1), 95–103.

Kroon, M., Wegdam, G. H., & Sprik, R. (1996). Dynamic light scattering studies on the sol-gel transition of a suspension of anisotropic colloidal particles. *Physical Review E, 54*(6), 6541–6550.

Lecomte, A., Dauger, A., & Lenormand, P. (2000). Dynamical scaling property of colloidal aggregation in a zirconia-based precursor sol during gelation. *Journal of Applied Crystallography, 33*(3–1), 496–499.

Li, L., Harnau, L., Rosenfeldt, S., & Ballauff, M. (2005). Effective interaction of charged platelets in aqueous solution: Investigations of colloid laponite suspensions by static light scattering and small-angle x-ray scattering. *Physical Review E, 72*, 051504.

Lin, S. H., Hsiao, R. C., & Juang, R. S. (2006). Removal of soluble organics from water by a hybrid process of clay adsorption and membrane filtration. *Journal of Hazardous Materials, 135*(1–3), 134–140.

Londoño, O. M., Tancredi, P., Rivas, P., Muraca, D., Socolovsky, L. M., & Knobel, M. (2018). Small angle X-ray scattering to analyze the morphological properties of nanoparticulated systems. In S. K. Sharma (Ed.), *Handbook of Materials Characterization* (pp. 37–75). Springer.

Luckham, P. F., & Rossi, S. (1999). The colloidal and rheological properties of bentonite suspensions. *Advances in Colloid and Interface Science, 82*(1–3), 43–92.

Martin, C., Pignon, F., Piau, J.-M., Magnin, A., Lindner, P., & Cabane, B. (2002). Dissociation of thixotropic clay gels. *Physical Review E, 66*, 021401.

Mihaila, S. M., Gaharwar, A. K., Reis, R. L., Khademhosseini, A., Marques, A. P., & Gomes, M. E. (2014). The osteogenic differentiation of SSEA-4 sub population of human adipose derived stem cells using silicate nanoplatelets. *Biomaterials, 35*(33), 9087–9099.

Mongondry, P., Tassin, J. F., & Nicolai, T. (2005). Revised state diagram of laponite dispersions. *Journal of Colloid and Interface Science, 283*(2), 397–405.

Mori, Y., Togashi, K., & Nakamura, K. (2001). Colloidal properties of synthetic hectorite clay dispersion measured by dynamic light scattering and small angle X-ray scattering. *Advanced Powder Technology, 12*(1), 45–59.

Mornet, S., Vasseur, S., Grasset, F., & Duguet, E. (2004). Magnetic nanoparticle design for medical diagnosis and therapy. *Journal of Materials Chemistry, 14*(14), 2161–2175.

Morvan, M., Espinat, D., Lambard, J., & Zemb, T. (1994). Ultrasmall and small angle X-ray scattering of smectite clay suspensions. *Colloids and Surfaces a: Physicochemical and Engineering Aspects, 82*(2), 193–203.

Mourchid, A., & Levitz, P. (1998). Long-term gelation of laponite aqueous dispersions. *Physical Review E, 57*(5), R4887–R4890.

Mourchid, A., Delville, A., Lambard, J., LeColier, E., & Levitz, P. (1995). Phase diagram of colloidal dispersions of anisotropic charged particles: Equilibrium properties, structure and rheology of laponite suspensions. *Langmuir, 11*(6), 1942–1950.

Mourchid, A., LéColier, E., Damme, H. V., & Levitz, P. (1998). On viscoelastic, birefringent, and swelling properties of

laponite clay suspensions: Revisited phase diagram. *Langmuir, 14*(17), 4718–4723.
Mousty, C. (2010). Biosensing applications of clay-modified electrodes: A review. *Analytical and Bioanalytical Chemistry, 396*, 315–325.
Neaman, A., & Singer, A. (2000). Rheology of mixed palygorskite-montmorillonite suspensions. *Clay and Clay Minerals, 48*(6), 713–715.
Nicolai, T., & Cocard, S. (2000). Light scattering study of the dispersion of laponite. *Langmuir, 16*(21), 8189–8193.
Pawar, N., & Bohidar, H. B. (2009). Hydrophobic hydration mediated universal self-association of colloidal nanoclay particles. *Colloids and Surfaces A: Physicochemical and Engineering Aspects, 333*(1–3), 120–125.
Permien, T., & Lagaly, G. (1994). The rheological and colloidal properties of bentonite dispersions in the presence of organic compounds IV. Sodium montmorillonite and acids. *Applied Clay Science, 9*(4), 251–263.
Pignon, F., Magnin, A., Piau, J. M., Cabane, B., Lindner, P., & Diat, O. (1997a). Yield stress thixotropic clay suspension: Investigations of structure by light, neutron, and x-ray scattering. *Physical Review E, 56*(3), 3281–3289.
Pignon, F., Magnin, A., & Piau, J. M. (1997b). Butterfly light scattering pattern and rheology of a sheared thixotropic clay gel. *Physical Review Letters, 79*(23), 4689–4692.
Pignon, F., Magnin, A., & Piau, J. M. (1998). Thixotropic behavior of clay dispersions: Combinations of scattering and rheometric techniques. *Journal of Rheology, 42*(6), 1349–1373.
Pujala, R. K., & Bohidar, H. B. (2013). Kinetics of anisotropic ordering in laponite dispersions induced by a water-air interface. *Physical Review E Statistical, Nonlinear, and Soft Matter Physics, 88*(5), 052310.
Pujala, R. K., & Bohidar, H. B. (2019). Hierarchical self-assembly, spongy architecture, liquid crystalline behavior and phase diagram of Laponite nanoplatelets in alcohol-water binary solvents. *Journal of Colloid and Interface Science, 554*, 731–742.
Pujala, R. K., Pawar, N., & Bohidar, H. B. (2011a). Unified scaling behavior of physical properties of clays in alcohol solutions. *Journal of Colloid and Interface Science, 364*, 311–316.
Pujala, R. K., Pawar, N., & Bohidar, H. B. (2011b). Universal sol state behavior and gelation kinetics in mixed clay dispersions. *Langmuir, 27*(9), 5193–5203.
Pujala, R. K., Joshi, N., & Bohidar, H. B. (2015). Spontaneous evolution of self-assembled phases from anisotropic colloidal dispersions. *Colloid and Polymer Science, 293*, 2883–2890.
Ramsay, J. D. F. (1986). Colloidal properties of synthetic hectorite clay dispersions: I. Rheology. *Journal of Colloid and Interface Science, 109*(2), 441–447.
Ramsay, J. D. F., & Lindner, P. (1993). Small-angle neutron scattering investigations of the structure of thixotropic dispersions of smectite clay colloids. *Journal of the Chemical Society, Faraday Transactions, 89*(23), 4207–4214.
Ranganathan, V. T., & Bandyopadhyay, R. (2017). Effects of aging on the yielding behavior of acid and salt induced laponite gels. *Colloids and Surfaces A: Physicochemical and Engineering Aspects, 522*, 304–309.
Rao, Y. (2010). Nanofluids: Stability, phase diagram, rheology and applications. *Particuology, 8*(6), 549–555.
Ravi Kumar, N. V. N., Muralidhar, K., & Joshi, Y. M. (2008). On the refractive index of ageing dispersions of laponite. *Applied Clay Science, 42*(1–2), 326–330.
Reffitt, D. M., Ogston, N., Jugdaohsingh, R., Cheung, H. F. J., Evans, B. A. J., Thompson, R. P. H., Powell, J. J., & Hampson, G. N. (2003). Orthosilicic acid stimulates collagen type 1 synthesis and osteoblastic differentiation in human osteoblast like cells in vitro. *Bone, 32*(2), 127–135.
Rodrigues, L. A. S., Figueiras, A., Veiga, F., de Freitas, R. M., Nunes, L. C. C., Filho, E. C. S., & Leite, C. M. S. (2013). The systems containing clays and clay minerals from modified drug release: A review. *Colloids and Surfaces b: Biointerfaces, 103*, 642–651.
Ruzicka, B., & Zaccarelli, E. (2011). A fresh look at the laponite phase diagram. *Soft Matter, 7*(4), 1268–1286.
Ruzicka, B., Zulian, L., & Ruocco, G. (2004). Routes to gelation in a clay suspension. *Physical Review Letters, 93*(25), 258301.
Ruzicka, B., Zulian, L., & Ruocco, G. (2006). More on the phase diagram of laponite. *Langmuir, 22*(3), 1106–1111.
Ruzicka, B., Zulian, L., Zaccarelli, E., Angelini, R., Sztucki, M., Moussaïd, A., & Ruocco, G. (2010). Competing interactions in arrested states of colloidal clays. *Physical Review Letters, 104*(8), 085701.
Sentenac, P., Lynch, R. J., Bolton, M. D., & Taylor, R. N. (2007). Alcohol's effect on the hydraulic conductivity of consolidated clay. *Environmental Geology, 52*, 1595–1600.
Sentenac, P., Ayeni, S., & Lynch, R. J. (2012). Effects of gasoline and diesel additives on kaolinite. *Environmental Earth Sciences, 66*, 783–792.
Seydibeyoglu, M., Demiroglu, S., Atagur, M., & Ocaktan, S. Y. (2017). Modification of clay crystal structure with different alcohols. *Natural Resources, 8*(11), 709–715.
Shahin, A., & Joshi, Y. M. (2010). Irreversible aging dynamics and generic phase behavior of suspensions of laponite. *Langmuir, 26*(6), 4219–4225.
Teh, E. J., Leong, Y. K., Liu, Y., Fourie, A. B., & Fahey, M. (2009). Differences in the rheology and surface chemistry of kaolin clay slurries: The source of the variations. *Chemical Engineering Science, 64*(17), 3817–3825.
Tomás, H., Alves, C. S., & Rodrigues, J. (2017). Laponite®: A key nanoplatform for biomedical applications? *Nanomedicine: Nanotechnology Biology, and Medicine, 14*(7), 2407–2420.
Wang, S., Wu, Y., Guo, R., Huang, Y., Wen, S., Shen, M., Wang, J., & Shi, X. (2013). Laponite nanodisks as an efficient platform for doxorubicin delivery to cancer cells. *Langmuir, 29*(16), 5030–5036.
Wu, Y., Guo, R., Wen, S., Shen, M., Zhu, M., Wang, J., & Shi, X. (2014). Folic acid-modified laponite nanodisks for targeted anticancer drug delivery. *Journal of Materials Chemistry B, 2*(42), 7410–7418.
Zhuang, Y., Zhao, L., Zheng, L., Hu, Y., Ding, L., Li, X., Liu, C., Zhao, J., Shi, X., & Guo, R. (2017). Laponite-polyethylenimine based theranostic nanoplatform for tumor-targeting CT imaging and chemotherapy. *ACS Biomaterials Science & Engineering, 3*(3), 431–442.

https://doi.org/10.1007/s42860-023-00229-5 Published online by Cambridge University Press